Data Analysis of Molecular Dications Fragmentation Processes by Double Photoionization with Synchrotron Radiation

Marco Parriani[1(✉)], Andrea Giustini[1], Michele Alagia[2], Robert Richter[3], Stefano Stranges[2,4], Raimund Feifel[5], and Stefano Falcinelli[1]

[1] Department of Civil and Environmental Engineering, University of Perugia, Via G. Duranti 93, 06125 Perugia, Italy
marco.parriani@dottorandi.unipg.it, {andrea.giustini, stefano.falcinelli}@unipg.it
[2] IOM CNR Laboratorio TASC, 34012 Trieste, Italy
alagia@iom.cnr.it, stefano.stranges@uniroma1.it
[3] Sincrotrone Trieste, Area Science Park, 34149 Basovizza, Trieste, Italy
robert.richter@elettra.trieste.it
[4] Department of Chemistry and Drug Technology, University of Rome Sapienza, 00185 Rome, Italy
[5] Department of Physics, University of Gothenburg, Origovägen 6B, 412 58 Gothenburg, Sweden
raimund.feifel@physics.gu.se

Abstract. In this paper is presented a summarizing description of the collection and computational analysis of the relevant data recorded following a double photoionization experiment on molecular species of interest in astrochemistry. In particular, the computational procedure used to analyze experimental data collected in the double photoionization of allene molecules by tunable radiation in the 25.0–45.0 photon energy range of the GASPHASE and CiPo beamlines of the ELETTRA synchrotron facility of Basovizza (Trieste, Italy) is outlined and discussed. Data presented are recorded using the ARPES (Angle Resolved PhotoEmission Spectroscopy) end station, which is a molecular beam apparatus coupled with a PEPIPICO (Photoelectron-Photoion-Photoion Coincidence) technique and TOF (Time-of-Flight) mass spectrometry, in three different beamtimes.

Keywords: photoionization · astrochemistry · dications

1 Introduction

1.1 Double Photoionization Studies

Ionic species are of great interest in astrochemistry and in planetary atmospheres [1–5], and they can be formed in space in various way, such as by chemi-ionization and photoionization [6–10]. In particular, the absorption of UV and EUV (Extreme

© The Author(s), under exclusive license to Springer Nature Switzerland AG 2024
O. Gervasi et al. (Eds.): ICCSA 2024 Workshops, LNCS 14818, pp. 55–70, 2024.
https://doi.org/10.1007/978-3-031-65273-8_4

Ultraviolet) photons and cosmic rays can induce multiple ionization with formation of doubly charged molecular species, which are called molecular dications. They were predicted to exist in the ionospheres of Mars, Venus and Titan, and then considerable amounts have been detected in such environments highlighting their relevant role, as for example, in the ion escape process from the atmosphere of Mars and Titan [11–15]. They were also found in interstellar clouds, comet tails and planetary ionospheres. Moreover, dications are involved in flames and plasma chemistry and physics [16]. The importance of coincidence studies of dications produced by the direct ejection of a couple of valence-shell electrons in determining the basic chemical properties of molecules has been pointed out by the pioneering work completed by J.H.D. Eland [17, 18]. In particular, the phenomenon of photoionization refers to the interaction of electromagnetic radiation with matter resulting in the dissociation of that matter into electrically charged particles [19, 20]. Our focus is studying the double photoionization of gas-phase small molecules producing dications that are important species involved in planetary ionospheres, astrochemistry and astrophysics [17–20], since they are optimal models for their simple and isolated structure, which permits to understand such a complex process as photoionization [21], in which several effects can play a major role.

Molecular dications fragmentation. Molecular dications have been subject of study due to their role in upper planetary atmosphere and interstellar medium, and in general for the role played in high energy environments [12–14]. We refer to double photoionization (DPI) as the process in which two electrons are removed simultaneously from an atom or a molecule by the absorption of a single photon, this leading to the formation of a dication (doubly charged atomic or molecular ion). Analysis of the emitted electrons and the ionic fragments produced by the dissociation of these dications makes it possible to extract fundamental information about the process, such as energy thresholds, kinetic energy releases (KERs) and angular distributions.

1.2 Electron-Ion-Ion Coincidence Measurements

A coincidence measurement is a method used to determine whether two or more particles originate from the same event to correlate them, when detecting the ion fragments emerged from the dissociation of multiply charged molecular ions. In a coincidence experiment the product ions and the photoelectrons emitted are detected and eventually correlated, providing a set of information on the energetic and mechanism of the photodissociation process. There are several different techniques developed during the years, based on the fundamental principle of measuring the arrival time of each charged particle [17]. In this paper will be presented an example of angle-resolved photoelectron spectroscopy (ARPES) setup, used by our group in collaboration with the staff of the GASPHASE and CiPo beamlines of the Elettra synchrotron facility, in Trieste, Italy.

2 Experimental Setup

2.1 The Allene Sample

Allene, C_3H_4, is the first member of the cumulene series C_nH_4. It is well known that allene and the other odd cumulenes belong to the D2d symmetry group, and exhibit stereoisomerism (axial chirality) [21]; The ground state electronic structure is of special interest since the HOMO level is doubly degenerate, having two helical shape Mos of opposite chirality [22]. It is thought to be present in the interstellar medium at least as an intermediate [23, 24], but as it lacks a dipole moment it has not yet been detected there directly. The data presented as example are the result of three different beam times performed at the Gas-phase and CiPo beamlines of the Elettra synchrotron facility (a detailed description of the beamline can be found at [25].

2.2 ARPES 3D Ion Imaging End Station

The ARPES end station used for the experimental measurements is an ion imaging spectroscopy apparatus, with a differential pumping system and the possibility to have two interchangeable molecular beam systems, a pyrolitic source and a hypodermic needle; This apparatus allows photoionization studies to be performed using a tunable and high photon flux of a third-generation synchrotron source. Such experimental studies were mainly based on the use of a PEPIPICO (PhotoElectron–PhotoIon–PhotoIon Coincidence) detector coupled with TOF (Time-of-Flight) mass spectrometer specially designed and built to measure the spatial momentum components of product fragments ions in the double photoionization experiments as we have done in the past [16, 23]. This specific endstation has been successfully used before applied to HX (where X = Cl, Br, and I) double photoionization experiments [6, 26, 27]. in the case of the allene, very recently, a detailed experimental and theoretical investigation of double and triple ionization, by single photon absorption, has been carried out [28], providing the energy pattern of dication electronic states, as well as some details on their nuclear dissociation dynamics. Our experimental investigation has been carried out at the GASPHASE beamline of the ELETTRA synchrotron facility of Basovizza (Trieste, Italy), using a synchrotron radiation in the 25.0 – 45.0 eV photon energy range to conduct a detailed study of the nuclear dissociation dynamics of allene dications by single photon valence electron double ionization by means of the 3D-ion imaging spectroscopy. This different multi-coincidence technique allows higher mass resolution and much higher sensitivity than before [28, 29], and allows to investigate metastable dissociation channels where ions differ by a single unit of mass. The investigated process can be schematized as follows below in Eq. (1):

$$C_3H_4 + hv \rightarrow (C_3H_4)^{2+} + 2e^- \rightarrow \text{fragment ions} \quad (1)$$

where, $(C_3H_4)^{2+}$ is the intermediate molecular dication of allene, which can lead to different species according to the relative position of the intermolecular potentials describing the fragment ion-ion and neutral doubly charged ion interactions characterizing the system [23]. In general, taking as an example the simple case of an AB^{2+} diatomic molecular

dication, three different cases can be distinguished, the case of the thermodynamically stable dications, the case of unstable species, that cannot be detected in gas phase, and the case of molecular dications in a metastable state, which are the result of an avoided crossing of the potential energy curves involved. In this third case, the resulting fragments A^+ and B^+ have in general a high relative kinetic energy release, with a process named Coulomb explosion of the metastable dication, leading to monocations with a translational energy content that range between 1–10 eV. In the case reported of allene, an analysis of metastable traces is shown in the data treatment section. The allene sample used was commercial as in previous experiments [28]; a stainless-steel needle has been used to introduce the sample into the chamber; in the experiment, the synchrotron radiation, with an energy range of 25–45 eV, passes through a monochromator, specifically a 400 lines/mm spherical grating in first order diffraction, with in and out slits adjusted to obtain a photon energy resolution of around 1.5 meV, and through a magnesium filter used to avoid spurious effects due to ionization by photons from higher orders of diffraction; then the radiation crosses the beam of the target molecule at the extraction region; the electrons are then accelerated towards a multi-channel plate (MCP) detector, and used as a trigger for the ions time of flight. Ions are extracted, accelerated towards a time of flight (TOF) spectrometer and mass selected. The photon flux crossing the target

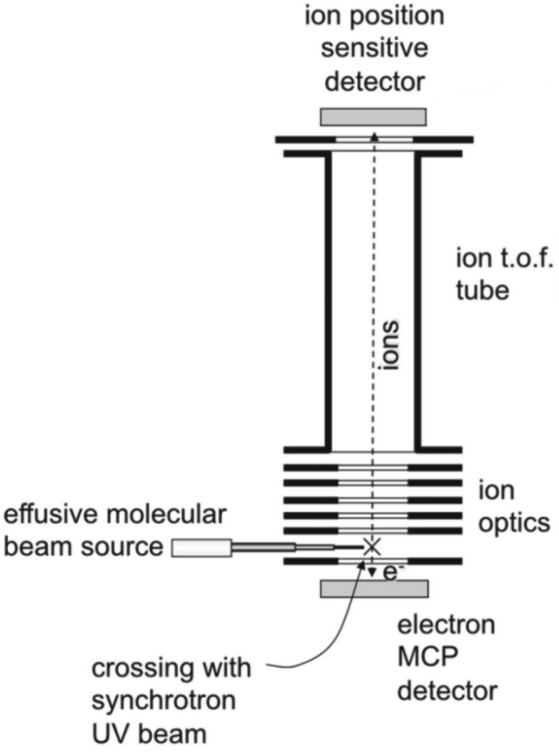

Fig. 1. Scheme of the experimental electron-ion-ion extraction and detection system installed in the ARPES Ion imaging spectrometer (MCP stands for multi-channel plate)

beam and the gas pressure are constantly monitored, thus ion yields are corrected for pressure and photon flux variations after every change in photon energy, moreover the gas inlet source is supplied with a mixture of the target molecule plus He, to allow the normalization of all ion signals at each photon energy to the total ion yield of helium. The ion impacts produce electron clouds collected by a position sensitive detector, which consists of 64 strip anodes (32 vertical and 32 horizontal), individually connected with an independent time-to-digital converter (TDC), allowing to measure several ion fragments and electrons from the same photoionization event. Moreover, a discriminator is connected to the 64 detectors. After an event, the signal is read from the TCD by a Versa Module Eurocard (VME) and sent to the acquisition computer which registers the data; specifically, every x and y of each particle hit is recorded, meaning that for each ion two space and one temporal coordinate are registered. The measured ions are also sorted in groups of single, double, triple,… Coincidences for every start electron [26]. The correlation can then be visualized by plotting a two-dimensional histogram, in which is usually reported the TOF of the first ion versus the TOF of the second ion (Fig. 3).Fig. 2.The coincidence plot recorded in the double photoionization of allene molecule at a photon energy of 30.0 eV (upper panel) and 40.8 eV (lower panel), as an example to appreciate the appearance of coincidence islands over the energy range used.

3 Data Analysis

By the double photoionization of allene using synchrotron radiation in the 25–45 eV photon energy range various fragmentation channel have been detected with the related energy threshold:

$$C_3H_4 + hv \rightarrow H^+ + C_3H^+ + H_2 + 2e^- \qquad hv \geq 30.0 \pm 0.1 \text{ eV} \tag{2}$$

$$H_2^+ + C_3H^+ + H + 2e^- \qquad hv \geq 30.0 \pm 0.1 \text{ eV} \tag{3}$$

$$H_3^+ + C_3H^+ + 2e^- \qquad hv \geq 30.0 \pm 0.1 \text{ eV} \tag{4}$$

$$H^+ + C_3H_2^+ + H + 2e^- \qquad hv \geq 35.0 \pm 0.1 \text{ eV} \tag{5}$$

$$H_2^+ + C_3H_2^+ + 2e^- \qquad hv \geq 34.0 \pm 0.1 \text{ eV} \tag{6}$$

$$H^+ + C_3H_3^+ + 2e^- \qquad hv \geq 27.8 \pm 0.1 \text{ eV} \tag{7}$$

$$CH^+ + C_2H_2^+ + 2e^- \qquad hv \geq 37.5 \pm 0.1 \text{ eV} \tag{8}$$

$$CH^+ + C_2H_3^+ + 2e^- \qquad hv \geq 33.0 \pm 0.1 \text{ eV} \tag{9}$$

$$CH_2^+ + C_2H^+ + 2e^- \qquad hv \geq 38.0 \pm 0.1 \text{ eV} \tag{10}$$

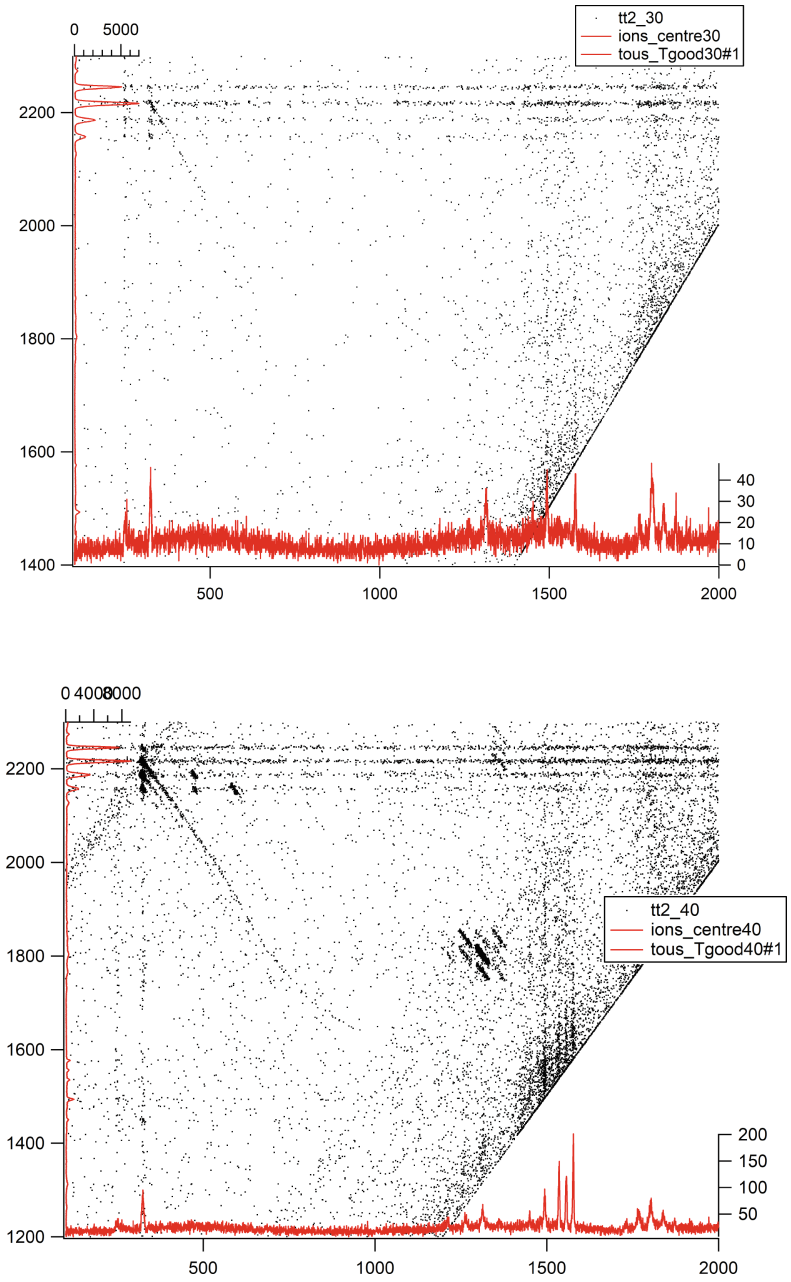

Fig. 2. The coincidence plot recorded in the double photoionization of allene molecule at a photon energy of 30.0 eV (upper panel) and 40.8 eV (lower panel), as an example to appreciate the appearance of coincidence islands over the energy range used.

$$CH_2^+ + C_2H_2^+ + 2e^- \qquad h\nu \geq 32.5 \pm 0.1 \text{ eV} \tag{11}$$

$$CH_3^+ + C_2H^+ + 2e^- \qquad h\nu \geq 33.5 \pm 0.1 \text{ eV} \tag{12}$$

The measured threshold energies reported above were obtained by accumulating for a minimum of 6–8 h at each investigated photon energy with a 200 meV photon energy step. Figure 2 reports the two time-of-flight of the corresponding ions and is usually referred as the coincidence map. It is possible to observe the so-called islands in correspondence of the time-of-flight crossing of two correlated ions; each specific dot in these islands represents a coincidence event and contains important information about the dynamics and kinetics of the dissociation process leading to the correlated ions [28]. Specifically, the slope and shape of the islands are related to the dissociation mechanism and energetics of the molecular ion photofragmentation, instead the intensity is directly related to the ionization probability of the molecular species and thus is fundamental to determine the photoionization thresholds and the appearing potentials of the fragments.

3.1 Ionization Thresholds

The threshold energies for each open ionization channel are usually enlightened by measuring the appearance of the so-called islands in the coincidences plot; the two time of flight values t_1 and t_2 define a point, since they are produced by the same photoionization event. By analyzing the number of events in a specific island over the energy range in which the measurements are performed (the case for allene is from 25 eV to 45 eV) one can investigate the appearance of various islands, related to the opening of the corresponding ionization channel, which can be deducted by the two peaks of the mass spectrum that are generating the island. Specifically, the procedure consists in defining the boundaries around the islands and obtaining the number of coincidences inside them; raw data are normalized over the total number of events detected over the time of the measurement, moreover these events need to be cleaned of the background, indeed in every coincidence experiment a random background is present, arising from false coincidences, random events that occur in the case of two not correlated stop signals, or for uncorrelated ion stop and electron start signals, this background usually depends to both electrons and ions counting rates. There are several methods to subtract this background [30], one of the simplest is to use a low counting rate with a long time measurement, but for the case of the detection of the ionization thresholds, in which a high counting rate is often necessary to avoid extremely long data acquisitions, one empirical method is to calculate the background in a relatively empty area of the plot, in which no event is taking place. Using the same island boundaries for the ionization channel detection and for the background calculation allows to empirically obtain the subtraction of false coincidences. Coincidence events are in every case normalized over photon flux to be comparable. It is important to say that in the case of allene, the normalization of raw data has not been done over the total number of events on the coincidence plot, this because a small portion of the spectrum, not overlapped in any case with important peaks, presented a recurring form in every spectrum at every energy; this was due to the fact that the MCP's used were nearly exhausted, so this particular shape was not

considered during the data treatment. To have a more fine detection, as in the case of the incipient formation of the molecular dication for allene, the variation in energy for each measurement has been varied on the order of the 200 meV, and the focus switched from the islands to the mass spectrum; this because the difference between the background and the events detected in the island becomes smaller, and it is more accurate to trying to identify the dication appearance by looking at the spectrum. Data collected has been then verified and confirmed by using a Wannier-based model to evaluate the experimental values for the ionization thresholds obtained. The evaluation of the threshold energy for the formation of $(C_3H_4)^{2+}$ allene dication confirmed the value reported in literature, which was 28 ± 0.3 eV. Specifically, we estimated an appearance energy value of 27.8 ± 0.1 eV for the allene dication, whose appearance can be more easily noticed through the observation of various coincidence plots over the energy range of 25.0–45.0 eV (graphic examples below and over the dication energy threshold are reported in Sect. 3.3).

3.2 Kinetic Energy Releases

The measurement of the impact coordinates and the arrival time for each particle investigated allows to calculate its linear momentum in the setup [24]:

$$p_{i,x} = p \sin\theta \cos\varphi = k_1\left(m\left(x_i - x_g\right)/t_i\right) \tag{13}$$

$$p_{i,y} = p \sin\theta \cos\varphi = k_1\left(m\left(y_i - y_g\right)/t_i\right) \tag{14}$$

$$p_{i,z} = p \cos\varphi = -k_2(t_i - t_0) \tag{15}$$

where x_g and y_g are the coordinates of the center of mass of the n-th PEPIPICO (photoelectron-photoion-photoion coincidence) dissociation event (z_g coordinate does not enter the equations if the WileyMacLaren time focusing is employed), m is the ion mass and t_0 is the arrival time for an ion with no initial momentum along the z axis, p is the magnitude of the momentum, θ and ϕ are respectively the polar and azimuth angles with respect to the radiation polarization vector; k_1 and k_2 are geometrical factors. If a complete two (or more) body dissociation is detected, we have enough measurements to solve the system of kinematical equations. In particular, one can calculate the x_g and y_g coordinates by applying the linear momentum conservation law, that is $\sum p_{i,x} = 0$ and $\sum p_{i,y} = 0$. The knowledge of the center of mass coordinates allows to transform the measured x_i, y_i, and t_i coordinates into the linear momenta components following the previous mentioned equations, and then the laboratory angles and energies can be computed. Thus, from the momenta distribution in the center of mass coordinate system it is possible to obtain the Total or Partial kinetic energy released (KER) in the dissociation process.

$$KER = p^2/2m \tag{16}$$

Angular distributions. Moreover, the photofragments angular distribution, with respect to the radiation polarization plane, can be obtained from the knowledge of the

ion momenta distribution and can provide valuable information about the dissociation dynamics according to Eq. 17:

$$I(\theta)\sin(\theta) = (\sigma_{tot}/4\pi)\,[1 + \beta/2\,(3\cos^2\theta - 1)] \tag{17}$$

in which I(θ) represent the differential cross section, θ is the angle between the velocity vector of the fragment ion and the light polarization vector, σ is the total cross section and β represent the anisotropy parameter; beta can assume different values, β = -1 if there is an emission of product ions along a direction perpendicular to the polarization vector, β = 0 if there is an isotropic distribution of fragment ions, β = 2 if there is an emission of product ions along a direction parallel to the polarization vector. In the case of the data taken as example, two data sets from two different experiments have been collected, the data reported in this paper are from the second data set: the first set refers to data taken with old MCPs in which their depletion caused the initial impossibility to determinate angular distributions, due to the appearance of a hole in the angular distribution of the fragments that could resemble an anisotropic distribution, misleading the analysis due to an incorrect estimation of the anisotropic parameter β. After the substitution of the old MCPs and the installation and conditioning of the new ones, several KERs have been measured over the energy range from 25.0 to 45.0 eV (with examples reported in Fig. 3 and 4), although there are no indications of an anisotropic distribution in the energy range we investigated. This can be highlighted by the estimation of the anisotropy parameter β, which is calculated through an iterative fit using Eq. 17. In our case of study, the best estimation of the parameter at different energies seems to confirm the absence of any anisotropic behavior in the energy range investigated. To examine a case in which an anisotropic distribution has been highlighted, the reader could refer to previous works as the one regarding propylene oxide [31], in which the best fit of experimental data was obtained using the sum of two different Gaussian functions highlighting a bimodality generated by the presence of two different reaction mechanisms. It is important to note that an important amount of the beamtime in which KERs have been measured has been devoted to low gain acquisitions to study the metastable tails originating from several fragmentation channels, for this reason the angular distribution for allene fragmentation could be a future, finer and deeply conducted investigation, to try adding more statistic to the study to further fortify the assumptions.

3.3 Metastable Lifetime

Doubly charged molecular dications are usually unstable species, because of their high formation energy. In the gas phase, the two charged parts of the dication tend to repel each other, making this specie in the majority of cases unstable, determining the fragmentation in two positive ions often with high KER; there are other cases in which the species can be metastable, leading to the formation of a so-called tail on the plot, indicating that the fragmentation reaction occurs in a time longer than the characteristic window time of the apparatus (in our case 50 ns). By analyzing the tail, it is possible to derive the lifetime for the dications leading to the dissociation reaction. In our case of study regarding allene, using a low gain acquisition for a minimum of 48 h, we collected data at an energy of 36.0 eV, energy in which we highlighted the presence of four distinct metastable tails,

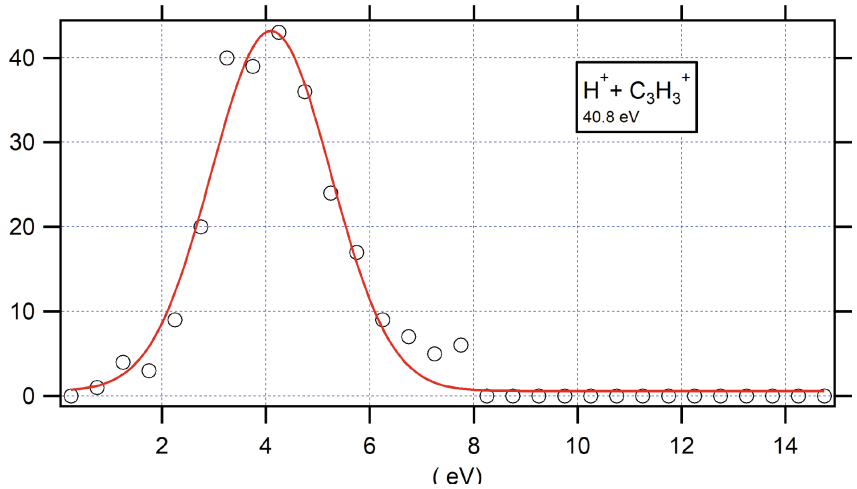

Fig. 3. A portion of the KER distribution for the production of $H^+ + C_3H_3{}^+$ ion pair products formed in the double dissociative photoionization of propylene oxide at a photon energy of 40.8 eV.

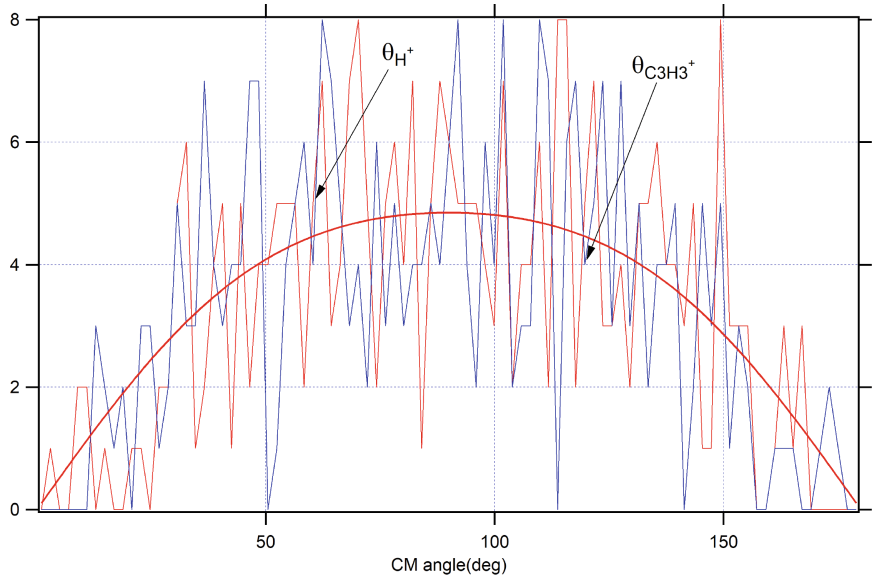

Fig. 4. The angular distribution of $H^+ + C_3H_3{}^+$ product ions in the center of the mass frame recorded at a photon energy of 40.8 eV, with an estimated $\beta = 0.15 \pm 0.13$.

reported in Figs. 5 and 6, originating from the fragmentation channels of Eqs. (2), (4), (5) and (7).

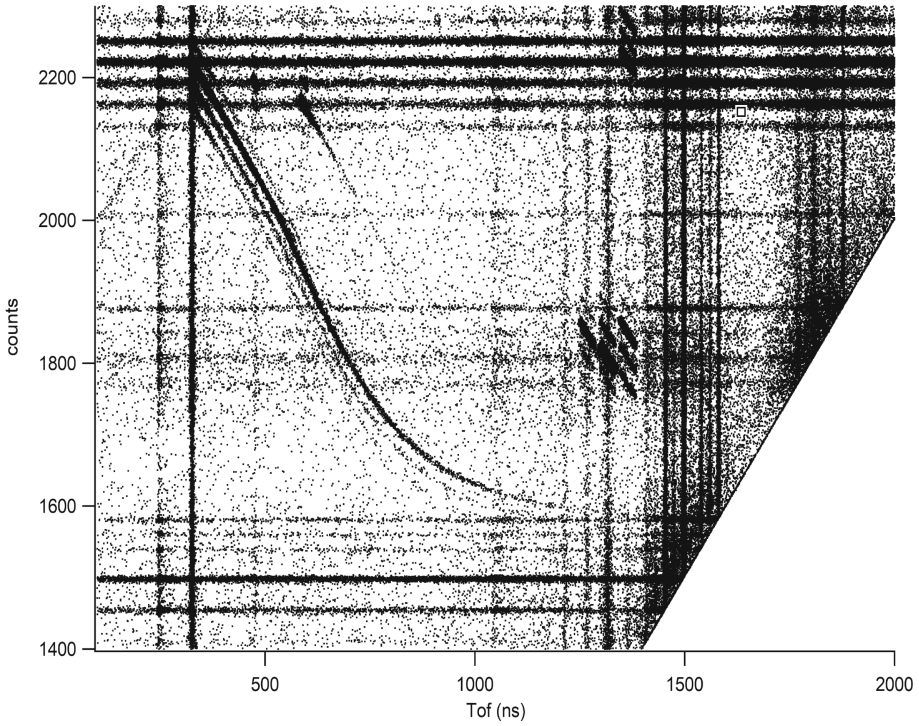

Fig. 5. The Coincidence plot collected with a low gain with a photon energy of 36 eV, to highlight the appearance of the metastable tails.

The plot has been analyzed to obtain the lifetime of the metastable dications during the dissociations. In the first place, a mask containing the trace has been created, to calculate all the events that laid inside the tail, and a background has been subtracted by translating the mask in an empty region of the coincidences plot to subtract the values inside it. To obtain the lifetime of the dications we have plotted the number of coincidence points along the track of the tails, as a function of the $(t_2 - t_1)$ difference and have fitted the data by a Monte Carlo simulation of the ion trajectories in the mass spectrometer. To give an example, the behavior for the $H^+ + C_3H_3{}^+ + 2e^-$ channel, with a photon energy of 36.0 eV, is reported in Fig. 7, where the dots are the experimental results, and the line is obtained with a simulation with 10^6 trajectories.

This way, the experimental data are compared with the best Monte Carlo fit simulation, and the reduced main square values χ^2 of the difference between experimental data and simulation are plotted as a function of the dication lifetime, the minimum obtained deviation gives the value we are looking for. In our case, a lifetime of 160 ± 20 ns resulted the best value to fit the experimental data; it is important to notice in any case that the Monte Carlo simulation we used is not able to perfectly fit the end of the metastable tail; while this does not seem to have a huge impact for the estimation of the lifetime of the main metastable tail, it could be of fundamental importance for the estimation of the weaker tails, especially for the one regarding the $H_3{}^+ + C_3H^+$ ion products, which

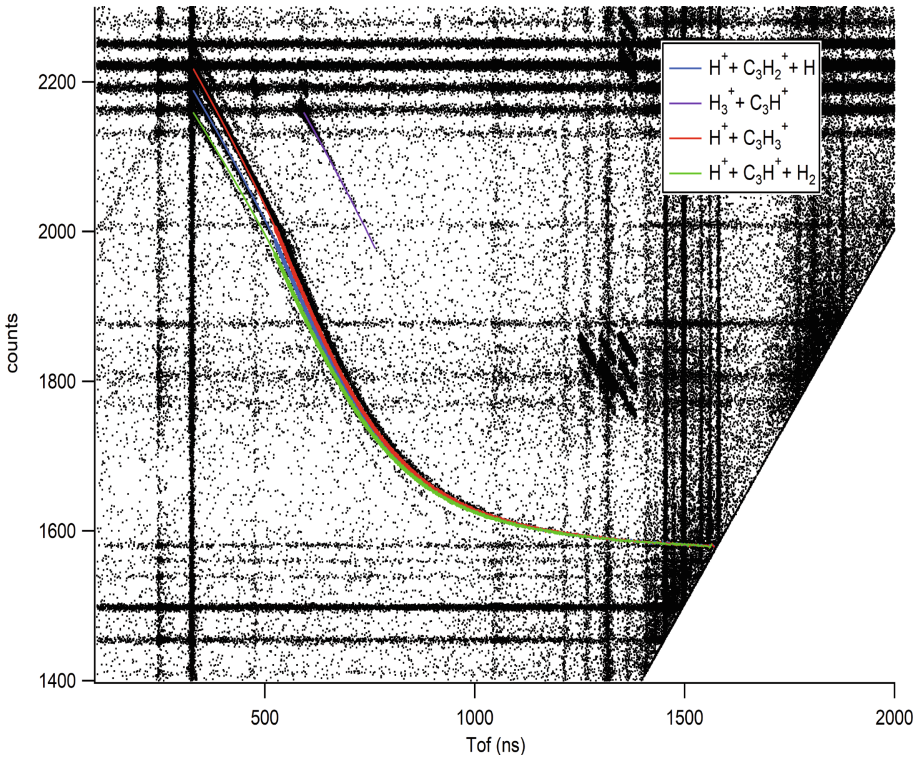

Fig. 6. The Coincidence plots collected with a low gain with a photon energy of 36 eV; the four different metastable tails simulated trajectories are highlighted with different colors.

is the weakest. For this reason, further studies to improve the simulation are currently ongoing to have a more precise estimation of the final part of the metastable tails. With the definition of the masks containing the coincidence events for the metastable tails, a scan from 25 to 45 eV has also been done to estimate the energy threshold formation for every metastable tail detected. In Fig. 8 the reader can appreciate the energy formation thresholds for the three main metastable tails (it is important to stretch that the metastable tail for the $H^+ + C_3H^+$ is very weak and thus it results difficult to determine with confidence the exact energy in which it appears, the same counts for the $H_3^+ + C_3H^+$ tail, which is also weaker and not reported below).

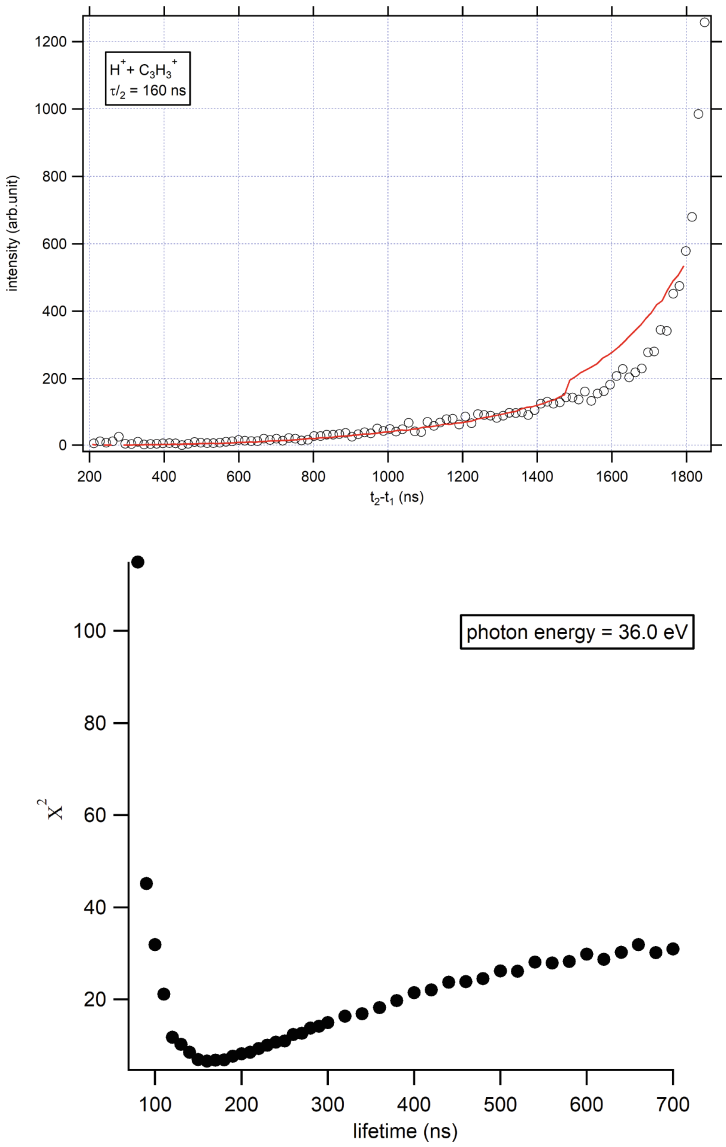

Fig. 7. Analysis of the main metastable tail in the coincidence plot of Fig. 5, in order to derive the lifetime of the dissociation reaction leading to $H^+ + C_3H_3{}^+$. The upper panel shows the intensity of coincidences along the tail track, as a function of the $t_2 - t_1$ difference (open circles), with the fit (continuous line) by a Monte Carlo trajectory calculation. The lower panel shows the reduced mean square deviation, χ^2, between the simulation and the experimental results, as a function of the lifetime used in the simulation.

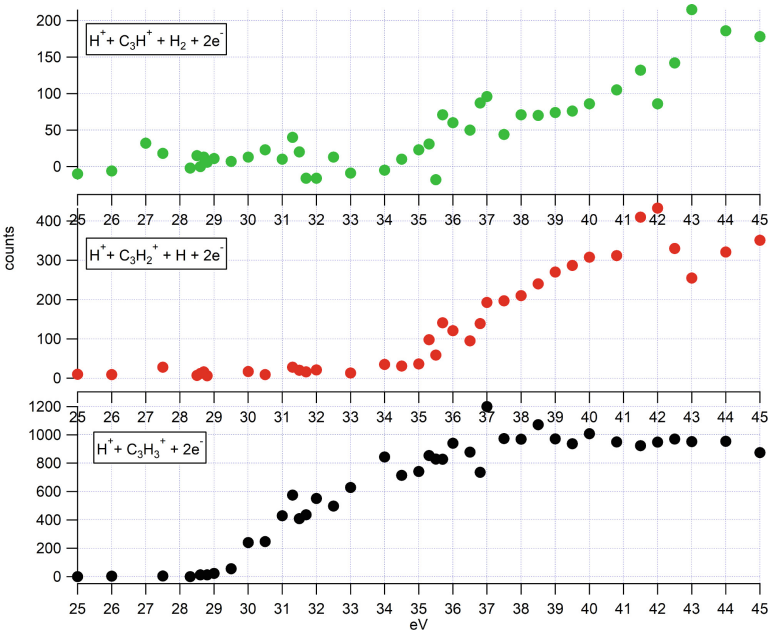

Fig. 8. The energy threshold formation for three of the four metastable tails highlighted, it is quite interesting that the tail referred to the $H^+ + C_3H^+$ ion products seems to start before the $H^+ + C_3H_2{}^+$ one; this cannot be said with a high level of confidence though, due to the high variability of the data and the weakness of the tail.

4 Conclusions

The experimental procedures we reported describe our apparatus and the data treatment we apply when performing a double photoionization experiment using a synchrotron light source; the example reported summarizes the different steps of the analysis, including the highlights of four different metastable tails. The experimental setup reported permits the measurement of cross sections for the different fragmentation channels together with kinetic energy releases and energy distributions, parameters that can be of great use to understand the chemistry of the ionosphere of our planet and other important bodies like Mars, Venus, or Titan. Further improvements to the data analysis could come from the use of a finer computational method for the analysis of the metastable tail, together with the collection of more statistic to allow a finer calculation of the energy distributions.

Acknowledgments. This work was supported and financed with the "Fondo Ricerca di Base, 2018, dell'Università degli Studi di Perugia" (Project Titled: Indagini teoriche e sperimentali sulla reattività di sistemi di interesse astrochimico). Support from Italian MIUR and University of Perugia (Italy) is acknowledged within the program "Dipartimenti di Eccellenza 2018–2022". The scientific staff of the GASPHASE beamline of ELETTRA Synchrotron Facility of Basovizza (Trieste, Italy) is warmly acknowledged.

References

1. Alagia, M., Balucani, N., Candori, P., Falcinelli, S., et al.: Production of ions at high energy and its role in extraterrestrial environments. Rend. Lincei Sci. Fisiche e Nat. **24**, 53–65 (2013)
2. Pei, L., Carrascosa, E., Yang, N., Falcinelli, S., Farrar, J.M.: Velocity map imaging study of charge-transfer and proton-transfer reactions of CH_3 radicals with H_3^+. J. Phys. Chem. Lett. **6**(9), 1684–1689 (2015)
3. Candori, P., Falcinelli, S., Pirani, F., Tarantelli, F., Vecchiocattivi, F.: Interaction components in the hydrogen halide dications. Chem. Phys. Lett. **436**(4–6), 322–326 (2007)
4. Stäuber, P., Doty, S.D., Van Dishoeck, E.F., Benz, A.O.: X-ray chemistry in the envelopes around young stellar objects. Astron. Astrophys. **440**(3), 949–966 (2005)
5. Thissen, R., Witasse, O., Dutuit, O., Wedlund, C.S., Gronoff, G., Lilensten, J.: Doubly-charged ions in the planetary ionospheres: a review. Phys. Chem. Chem. Phys. **13**(41), 18264–18287 (2011)
6. Biondini, F., Brunetti, B.G., Candori, P., De Angelis, F., et al.: Penning ionization of N_2O molecules by He*($2^{3,1}S$) and Ne*($^3P_{2,0}$) metastable atoms: Theoretical considerations about the intermolecular interactions. J. Chem. Phys. **122**(16), 164308 (2005)
7. Biondini, F., Brunetti, B.G., Candori, P., De Angelis, F., et al.: Penning ionization of N_2O molecules by He*($2^{3,1}S$) and Ne*($^3P_{2,0}$) metastable atoms: crossed beam study. J. Chem. Phys. **122**(16), 164307 (2005)
8. Brunetti, B., Candori, P., De Andres, J., Pirani, F., et al.: Dissociative ionization of methyl chloride and methyl bromide by collision with metastable neon atoms. J. Phys. Chem. A **101**(41), 7505–7512 (1997)
9. Bartocci, A., Belpassi, L., Cappelletti, D., Falcinelli, S., et al.: Catching the role of anisotropic electronic distribution and charge transfer in halogen bonded complexes of noble gases. J. Chem. Phys. **142**(18), 184304 (2015)
10. Brunetti, B.G., Candori, P., Falcinelli, S., Pirani, F., Vecchiocattivi, F.: The stereodynamics of the Penning ionization of water by metastable neon atoms. J. Chem. Phys. **139**(16), 164305 (2013)
11. Gronoff, G., et al.: Modelling dications in the diurnal ionosphere of Venus. Astron. Astrophys. **465**(2), 641–645 (2007)
12. Falcinelli, S., et al.: Kinetic energy release in molecular dications fragmentation after VUV and EUV ionization and escape from planetary atmospheres. Plan. Space Sci. **99**, 149–157 (2014)
13. Falcinelli, S., et al.: The escape of O^+ ions from the atmosphere: an explanation of the observed ion density profiles on Mars. Chem. Phys. Lett. **666**, 1–6 (2016)
14. Falcinelli, S., Pirani, F., Vecchiocattivi, F.: The possible role of penning ionization processes in planetary atmospheres. Atmosphere **6**(3), 299–317 (2015)
15. Falcinelli, S.: Mass spectrometric detection of alkaline earth monohalide dications. Mol. Phys. **88**(3), 663–672 (1996)
16. Falcinelli, S., Rosi, M.: Production and characterization of molecular dications: experimental and theoretical efforts. Molecules **25**, 4157 (2020)
17. Eland, J.H.D.: The dynamics of three-body dissociations of dications studied by the triple coincidence technique PEPIPICO. Mol. Phys. **61**(3), 725–745 (1987)
18. Price, S.D., Eland, J.H.D., Fournier, P.G., Fournier, J., Milli´e, P.: Electronic states and decay mechanisms of the N_2O^{2+} dication. J. Chem. Phys. **88**, 1511–1515 (1988)
19. Houfner, S.: Photoelectron Spectroscopy: principles and applications, 3rd edn. Springer-Verlag, Berlin Heidelberg (2013)
20. Oswald, S.: X-ray Photoelectron Spectroscopy in Analysis of Surfaces, Encyclopedia of Analytical Chemistry (2006)

21. Hendon, C.H., Tiana, D., Murray, A.T., Carbery, D.R., Walsh, A.: Helical frontier orbitals of conjugated linear molecules. Chem. Sci. **4**(11), 4278–4284 (2013)
22. Garner, M.H., Hoffmann, R., Rettrup, S., Solomon, G.C.: Coarctate and mobius: the helical orbitals of allene and other cumulenes. ACS Central Sci. **4**(6), 688–700 (2018)
23. Falcinelli, S., et al.: Double photoionization of propylene oxide: a coincidence study of the ejection of a pair of valence-shell electrons. J. Chem. Phys. **148**(11), 114302 (2018)
24. Kaiser, R.I., Stranges, D., Lee, Y.T., Suits, A.G.: Neutral-neutral reactions in the interstellar medium. I. Formation of carbon hydride radicals via reaction of carbon atoms with unsaturated hydrocarbons. Astrophys. J. **477**(2), 982 (1997)
25. Derossi, A., Lama, F., Piacentini, M., Prosperi, T., Zema, N.: High flux and high-resolution beamline for elliptically polarized radiation in the vacuum ultraviolet and soft X-ray regions. Rev. Sci. Instrum. **66**, 1718–1720 (1995)
26. Lavollée, M.: A new detector for measuring three-dimensional momenta of charged particles in coincidence. Rev. Sci. Instrum. **70**(7), 2968–2974 (1999)
27. Alagia, M., et al.: The double photoionization of HCl: an ion–electron coincidence study. J. Chem. Phys. **121**(21), 10508–10512 (2004)
28. Ideböhn, V., Sterling, A.J., Wallner, M., et al.: Phys. Chem. Chem. Phys. **24**, 786–796 (2022)
29. Eland, J.H.D.: Dynamics of fragmentation reactions from peak shapes in multiparticle coincidence experiments. Laser Chem. **11**, 259 (1991)
30. Frasinski, L.J., Stankiewicz, M., Haterly, P.A., Codling, K.: Removal of false coincidences in triple coincidence experiments employing continuous excitation. Meas. Sci. Technol. **3**, 1188 (1992)
31. Falcinelli, S., et al.: Angular distribution of ion products in the double photoionization of propylene oxide. Front. Chem. **7**, 621 (2019)